

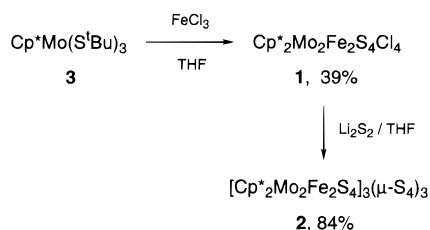
Construction of a Cyclic Tricubane Cluster [Cp*₂Mo₂Fe₂S₄Cl₂]₃(μ-S₄)₃ from the Mo₂Fe₂S₄ Single Cubane Component

Hiroyuki Kawaguchi, Kazuhiro Yamada, Shiho Ohnishi, and Kazuyuki Tatsumi*

Department of Chemistry, Graduate School of Science, Nagoya University
Furo-cho, Chikusa-ku, Nagoya 464, Japan

Received July 14, 1997

Over the past two decades, extensive efforts have been made to synthesize mixed-metal sulfido clusters of high nuclearity, and exploitation of new cluster components continues to be an imperative step for accomplishing unprecedented arrangements of large core structures.¹ In particular, construction of clusters containing iron and/or molybdenum is one of the major objectives in this field. Although spontaneous self-assembly has been a dominant strategy for the synthesis of such clusters,² more rational approaches to aggregation of cluster units have also emerged.³ For instance, dicubane clusters [(Fe₄S₄Cl₃)₂(μ-S)]⁴⁻, [(MoFe₃S₄Cl₂(Cl₄cat))₂(μ-S)₂]⁶⁻, and [(MoFe₃S₄Cl₂(Cl₄cat))₂(μ-S)(μ-L)]ⁿ⁻ (L = N₂H₄, n = 4; L = CN, OH, n = 5) were prepared by treating the corresponding single cubane complexes with Na₂S, (Et₄N)₂S, and NEt₄OH/L₂S.^{4,5} Recently, it was reported that reaction of [Fe₄S₄Cl₄]²⁻ with PR₃ and subsequent reduction resulted in fusion of two and four cubane cores.^{6,7} In this paper, we report the synthesis of a new class of Mo₂Fe₂S₄ cubane complex, Cp*₂Mo₂Fe₂S₄Cl₂ (**1**; Cp* = η⁵-C₅Me₅), and the formation of a novel cyclic tricubane cluster [Cp*₂Mo₂Fe₂S₄]₃(μ-S₄)₃ (**2**), from the reaction of **1** with Li₂S₂.



We previously reported a C–S bond cleaving reaction of Cp*Mo(S'Bu)₃ (**3**) leading to a Mo(VI) thio/thiolate complex,

(1) (a) Dance, I.; Fisher, K. *Prog. Inorg. Chem.* **1994**, *41*, 637–803. (b) Routledge, C. A.; Humanes, M.; Li, Y.-J.; Sykes, A. G. *J. Chem. Soc., Dalton Trans.* **1994**, 1274–1282. (c) Shibahara, T. *Coord. Chem. Rev.* **1993**, *123*, 73–147. (d) Coucouvanis, D. *Acc. Chem. Res.* **1981**, *14*, 201–209. (e) Müller, A.; Diemann, E.; Jostes, R.; Bögge, H. *Angew. Chem., Int. Ed. Engl.* **1981**, *20*, 934–955.

(2) (a) Nordlander, E.; Lee, S. C.; Cen, W.; Wu, Z. Y.; Natoli, C. R.; Di Cicco, A.; Filippini, A.; Hedman, B.; Hodgson, K. O.; Holm, R. H. *J. Am. Chem. Soc.* **1993**, *115*, 5549–5558. (b) Holm, R. H. *Adv. Inorg. Chem.* **1992**, *38*, 1–71. (c) You, J.-F.; Snyder, B. S.; Papaefthymiou, G. C.; Holm, R. H. *J. Am. Chem. Soc.* **1990**, *112*, 1067–1076. (d) Holm, R. H.; Simhon, E. D. In *Molybdenum Enzymes*; Spiro, T. G., Ed.; Wiley-Interscience: New York, 1985; Chapter 1. (e) Holm, R. H. *Chem. Soc. Rev.* **1981**, *10*, 455–490.

(3) Coucouvanis, D. *Acc. Chem. Res.* **1991**, *24*, 1–8.

(4) Challen, P. R.; Koo, S.-M.; Dunham, W. R.; Coucouvanis, D. *J. Am. Chem. Soc.* **1990**, *112*, 2455–2456.

(5) (a) Challen, P. R.; Koo, S.-M.; Kim, C. G.; Dunham, W. R.; Coucouvanis, D. *J. Am. Chem. Soc.* **1990**, *112*, 8606–8607. (b) Coucouvanis, D.; Challen, P. R.; Koo, S.-M.; Davis, W. M.; Butler, W.; Dunham, W. R. *Inorg. Chem.* **1989**, *28*, 4181–4183.

(6) Goh, C.; Segal, B. M.; Huang, J.; Long, J. R.; Holm, R. H. *J. Am. Chem. Soc.* **1996**, *118*, 11844–11853.

(7) (a) The reaction of (NEt₄)₂[MoFe₃S₄Cl₃(Cl₄cat)(CH₃CN)] with NaBPh₄ (or NaPF₆) in the presence of PR₃ was reported to give the edge-linked double cubanes Mo₂Fe₆S₈(PR₃)₆(Cl₄cat)₂: Demadis, K. D.; Campana, C. F.; Coucouvanis, D. *J. Am. Chem. Soc.* **1995**, *117*, 7832–7833. (b) It was reported that treatment of [Fe₄S₄(ArNC)₉] with KBAr₄ afforded [(Fe₄S₄(ArNC)₉)₂][BAr₄]₂: Harmjan, M.; Saak, W.; Haase, D.; Pohl, S. *J. Chem. Soc., Chem. Commun.* **1997**, 951–952.

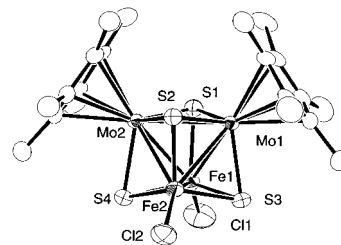


Figure 1. The structure of Cp*₂Mo₂Fe₂S₄Cl₂ (**1**) showing 50% thermal ellipsoids. Selected bond distances (Å): Mo1–Mo2 2.8219(7), Mo1–Fe1 2.760(1), Mo1–Fe2 2.761(1), Mo2–Fe1 2.753(1), Mo2–Fe2 2.754(1), Fe1–Fe2 2.791(1), Fe1–Cl1 2.180(3), Fe2–Cl2 2.197(2), Mo–S av 2.332, Fe–S av 2.263.

Cp*Mo(S)₂(S'Bu).⁸ This reaction was facilitated by oxidants such as S₈ and grey selenium, and we anticipated that FeCl₃ would promote C–S bond cleavage as well. Thus, the complex **3** was treated with 1 equiv of FeCl₃ in THF to give immediately a dark red solution, and a further color change was noticed when the solution was stirred at room temperature for 12 h. Removal of the solvent and recrystallization of the resulting solid from CH₂Cl₂/hexane generated an unexpected tetranuclear cluster Cp*₂Mo₂Fe₂S₄Cl₂ (**1**) as black crystals in 39% yield.⁹ The combustion analysis was in agreement with the formula, and the ¹H NMR spectrum in CDCl₃ showed a broad singlet at 1.81 ppm (Cp*, the width at half-height ν_{1/2} = 33 Hz) indicating a weak paramagnetic nature of the compound. According to the cyclic voltammetric experiment, one reversible redox couple appears at –0.88 V (E_{1/2} vs SCE) and one irreversible oxidation occurs at 1.14 V (E_p vs SCE).¹⁰ While there is uncertainty in defining oxidation states of the metal components, a plausible allotment may be Mo(IV) + Fe(II). Then reduction of iron from Fe(III) to Fe(II) is considered to occur during the cluster formation with the concomitant C–S bond breaking process.

As shown in Figure 1, the X-ray analysis revealed that complex **1** consists of a distorted Mo₂Fe₂S₄ cubane core. Two Cp* ligands and two Cl atoms further coordinate at the molybdenum and the iron sites, respectively.¹¹ Alternatively, the core structure can be viewed as a Mo₂Fe₂ tetrahedron face-capped by four sulfur atoms. While the main structural feature of **1** resembles closely that of Cp'₂Mo₂Fe₂S₄(NO)₂ (**4**; Cp' = η⁵-C₅Me₄Et),^{12a} their electron counts are different. The latter complex **4** is an electron-precise system with 60 cluster electrons,^{13,14} and the four metal atoms are connected through direct metal–metal single bonds. On the other hand, the Mo₂–Fe₂ tetrahedral core of **1** carries 56 electrons, i.e., 4 electrons less than **4**, which is consistent with paramagnetism of the cluster. The electron-deficiency of **1** affects the Fe–Fe distance most significantly, being 0.087 Å longer than that of **4**. The

(8) Kawaguchi, H.; Yamada, K.; Lang, J.; Tatsumi, K. *J. Am. Chem. Soc.* **1997**, *119*, 10346–10358.

(9) For Cp*₂Mo₂Fe₂S₄Cl₂ (**1**): ¹H NMR (CDCl₃) δ 1.81 (br, s, ν_{1/2} = 33 Hz); UV–vis (THF) λ_{max} (ε, M⁻¹ cm⁻¹) 299 (20 000), 459 (1600), 551 (760), 603 (530) nm. Anal. Calcd for C₂₀H₃₀S₄Mo₂Fe₂Cl₂: C, 31.07; H, 3.91; S, 16.59. Found: C, 30.92; H, 3.91; S, 16.28.

(10) The cyclic voltammograms of **1** and **2** were recorded in THF solution on a glassy carbon electrode with Bu₄NClO₄ as the supporting electrolyte. The potentials are reported vs saturated calomel electrode, SCE.

(11) Crystal data for Cp*₂Mo₂Fe₂S₄Cl₂ (**1**): monoclinic, P2₁/n (No. 14), a = 9.526(2) Å, b = 14.997(2) Å, c = 18.917(3) Å, β = 95.97(1)°, V = 2688.8(8) Å³, Z = 8, D_c = 1.910 g/cm³, 2θ_{max} = 50.0°, 5260 measured reflections of which 3755 with I > 3.00σ(I) were used for the refinement to give R = 0.036, R_w = 0.049, and GOF = 1.92.

(12) (a) Mansour, M. A.; Curtis, M. D.; Kampf, J. W. *Organometallics* **1997**, *16*, 275–284. (b) Recently, (C₅Me₄Et)₂Mo₂Co₂S₄X₂ (X = Cl, Br, I) were reported: Mansour, M. A.; Curtis, M. D.; Kampf, J. W. *Organometallics* **1997**, *16*, 3363–3370.

(13) (a) Trinh-Toan; Teo, B. K.; Ferguson, J. A.; Meyer, T. J.; Dahl, L. F. *J. Am. Chem. Soc.* **1977**, *99*, 408–416. (b) Bottomley, F.; Grein, F. *Inorg. Chem.* **1982**, *21*, 4170–4178. (c) Mingos, D. M. P. *Chem. Soc. Rev.* **1986**, *15*, 31–61.

(14) Harris, S. *Polyhedron* **1989**, *8*, 2843–2882.

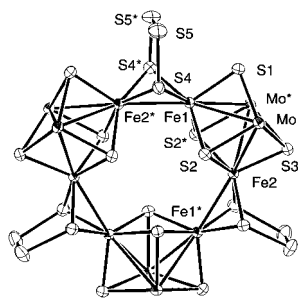


Figure 2. The structure of $[\text{Cp}^*_2\text{Mo}_2\text{Fe}_2\text{S}_4]_3(\mu\text{-S}_4)_3$ (**2**) showing 50% thermal ellipsoids; Cp* groups are omitted for clarity. Selected bond distances (Å) and angles (deg): Mo–Mo* 2.760(2), Mo–Fe1 2.802(2), Mo–Fe2 2.800(2), Fe1–Fe2* 2.610(3), Mo–S1 2.325(3), Mo–S2 2.296(3), Mo–S3 2.325(2), Fe1–S1 2.197(4), Fe1–S2 2.267(3), Fe1–S4 2.213(3), Fe2–S2 2.163(3), Fe2–S3 2.193(4), Fe2–S4* 2.214(3), Fe1–S4–Fe2* 72.2(1), S4–Fe1–S4* 83.4(1).

Mo–Mo distance of 2.8219(7) Å and the mean Mo–Fe bond length of 2.757 Å are both comparable to the corresponding distances of **4** (Mo–Mo, 2.8419(7) Å; Mo–Fe, 2.7654(7) Å). Although various $\text{M}_2\text{M}'_2\text{S}_4$ clusters having cyclopentadienyl auxiliaries are known,^{12,14,15} most of them were procured with π -acceptor ligands such as CO and NO. Thus, a unique feature of **1** is chloride ligation to each iron atom, which has the advantage of serving as a potential building unit for the synthesis of polycubane cluster aggregate.

The aggregation of **1** was accomplished by treating it with dry Li_2S_2 in THF,¹⁶ and an unprecedented tricubane cluster $[\text{Cp}^*_2\text{Mo}_2\text{Fe}_2\text{S}_4]_3(\mu\text{-S}_4)_3$ (**2**) was isolated as black crystals in 84% yield by recrystallization from toluene.¹⁷ The Mo:Fe:S ratio of 1:1:4 was consistent with the X-ray fluorescence microanalysis, and the molecular structure was determined by the X-ray analysis, where the crystals were found to be solvated by toluene.¹⁸ Three $\text{Mo}_2\text{Fe}_2\text{S}_4$ cubane skeletons are linked by three $\mu_2, \eta^2\text{-S}_4(2-)$ ligands, as shown in Figure 2. Each $\text{S}_4(2-)$ ligand bridges two Fe atoms of different cubanes, which is situated perpendicular to the Fe–Fe vector. Being crystallized in the hexagonal $P6_3/m$ space group, the molecule has crystallographic D_{3h} symmetry. A C_3 axis runs through the center of molecule, and all Fe atoms and six cubane S atoms, S1 and S3, lie in a mirror plane. Within each cubane core, the Mo–Mo distance is 0.06 Å shorter than that of **1**, and Mo–Fe distances are elongated by 0.04 Å. Most significant difference between the cubane geometries of **1** and **2** is that there is no direct Fe–Fe interaction for **2** and the iron atoms are separated by 3.235(2) Å. Instead, a new intercubane Fe–Fe bond is formed with the distance of 2.610(3) Å. As this intercubane Fe–Fe bonding is taken into account, the tetrahedral Mo_2Fe_2 unit has 62 cluster electrons, and the consequence is the long Fe–Fe distance within the cubane simply because the extra two electrons must reside in an antibonding molecular orbital.^{12,19,20} It is of interest to

(15) (a) Wachter, J. *Angew. Chem., Int. Ed. Engl.* **1989**, *28*, 1613–1626. (b) Cowans, B. A.; Haltiwanger, R. C.; Rakowski DuBois, M. *Organometallics* **1987**, *6*, 995–1004.

(16) Tatsumi, K.; Inoue, Y.; Kawaguchi, H.; Kohsaka, M.; Nakamura, A.; Cramer, R.; VanDoorne, W.; Taogoshi, G. J.; Richmann, P. N. *Organometallics* **1993**, *12*, 352–364.

(17) For $[\text{Cp}^*_2\text{Mo}_2\text{Fe}_2\text{S}_4]_3(\mu\text{-S}_4)_3$ (**2**): $^1\text{H NMR}$ (C_6D_6) δ 1.93 (s); UV–vis (THF) λ_{max} (ϵ , $\text{M}^{-1}\text{cm}^{-1}$) 412 (30 000), 470 (5800), 645 (2900) nm. Anal. Calcd for $\text{C}_{67}\text{H}_{98}\text{S}_{24}\text{Mo}_6\text{Fe}_6$: C, 31.15; H, 3.82; S, 29.78. Found: C, 31.47; H, 4.19; S, 30.95.

(18) Crystal data for $[\text{Cp}^*_2\text{Mo}_2\text{Fe}_2\text{S}_4]_3(\mu\text{-S}_4)_3\cdot\text{C}_7\text{H}_8$ (**2**): hexagonal, $P6_3/m$ (No. 176), $a = 16.264(8)$ Å, $c = 19.949(6)$ Å, $V = 4572(3)$ Å³, $Z = 2$, $D_c = 1.877$ g/cm³, $2\theta_{\text{max}} = 55.0^\circ$, 2109 measured reflections of which 1305 with $I > 3.00\sigma(I)$ were used for the refinement to give $R = 0.043$, $R_w = 0.054$, and GOF = 1.87.

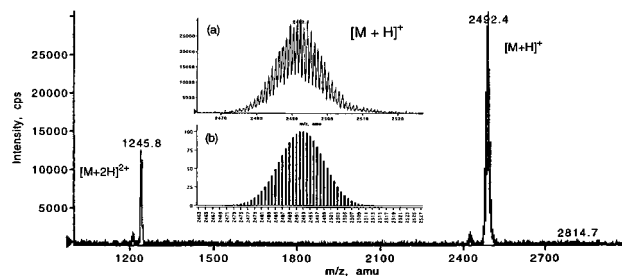
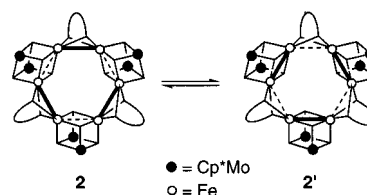


Figure 3. Positive electrospray ionization mass spectrum of $[\text{Cp}^*_2\text{Mo}_2\text{Fe}_2\text{S}_4]_3(\mu\text{-S}_4)_3$ (**2**). The inset shows (a) an expansion of the $2 + \text{H}^+$ peaks and (b) the calculated isotopic distribution of the ion.

Scheme 1



propose another Fe–Fe σ -bond alternation geometry **2'** as illustrated in Scheme 1. If the intercubane Fe–Fe bond is cleaved, then the Mo_2Fe_2 core becomes electron precise and the intracubane Fe–Fe bond would be formed. This bond isomer **2'** should electronically be feasible,^{20,21} and a certain electronic perturbation may induce transformation from the observed structure **2** to **2'**.

As one would expect from the above electron count, the tricubane cluster **2** is diamagnetic, and the Cp* proton signal appears at 1.93 ppm as a sharp singlet in the $^1\text{H NMR}$ spectrum. Interestingly, **2** is quite soluble in toluene and THF in spite of the large size of the cluster. The UV–vis spectrum in toluene exhibits a characteristic absorption at 412 nm, while the spectrum of **1** is featureless. The redox property of **2** also differs from **1**, and it is characterized by three reversible redox couples at 0.69, 0.26, and -0.11 V ($E_{1/2}$ vs SCE) and one irreversible reduction step at -0.85 V (E_p vs SCE).¹⁰ The electrospray ionization mass (ESI) spectrometry, carried out by adding a small amount of acetic acid to a THF solution of **2**, deserves comment.²² The positive ion ESI spectrum, provided in Figure 3, clearly shows two sets of ion peaks associated with mono- and di-protonated species, $[\text{M} + \text{H}]^+$ and $[\text{M} + 2\text{H}]^{2+}$, with the correct isotope distributions. The tricubane structure is readily protonated under the mass condition, and such species might well be generated in a preparative scale. Further study of reactivity of **1** and **2** is currently underway.

Supporting Information Available: Experimental procedures and a table listing data for crystal data, atomic coordinates, bond lengths and angles, and anisotropic displacement parameters for **1** and **2** (24 pages). See any current masthead page for ordering and Internet access instructions.

JA972330Y

(19) (a) Koide, Y.; Bautista, M. T.; White, P. S.; Schauer, C. K. *Inorg. Chem.* **1992**, *31*, 3690–3692. (b) Inomata, S.; Tobita, H.; Ogino, H. *Inorg. Chem.* **1992**, *31*, 722–723. (c) Lockemeyer, J. R.; Rauchfuss, T. B.; Rheingold, A. L. *J. Am. Chem. Soc.* **1989**, *111*, 5733–5738. (d) Bedard, R. L.; Dahl, L. F. *J. Am. Chem. Soc.* **1986**, *108*, 5933–5942.

(20) Houser, E. J.; Rauchfuss, T. B.; Wilson, S. R. *Inorg. Chem.* **1993**, *32*, 4069–4076 and references therein.

(21) Chisholm, M. H.; Clark, D. L.; Hampden-Smith, M. J. *J. Am. Chem. Soc.* **1989**, *111*, 574–586.

(22) The electrospray mass spectrum was obtained on a Perkin-Elmer API 300 mass spectrometer.